

# Performance Analysis of a System using Coordinate Interleaving and Constellation Rotation in Frequency-Selective Fading Channels

Nauman F. Kiyani

Faculty of Electrical Engineering  
Mathematics and Computer Science  
Delft University of Technology  
2600 GA Delft, The Netherlands  
Email: n.f.kiyani@tudelft.nl

Jos H. Weber

Faculty of Electrical Engineering  
Mathematics and Computer Science  
Delft University of Technology  
2600 GA Delft, The Netherlands  
Email: j.h.weber@tudelft.nl

**Abstract**—Performance analysis of a system employing coordinate interleaving and constellation rotation in frequency-selective fading channels is presented. The achievable performance for  $L$ -branch microdiversity using maximum ratio combining (MRC) receiver is analyzed and an upper bound on the average probability of bit error ( $P_b$ ) is presented. Exact closed form expressions for pairwise error probability (PEP) are derived for single-symbol transmission in a multipath fading environment. It is shown that the derived upper bound is tight for high signal-to-noise ratios (SNR). The optimum rotation angles are found by minimizing the upper bound and it is shown that the optimum rotation angles change as the number of diversity branches is increased. Furthermore the effect of different signal constellation mappings on the system performance is also presented and it is shown that the Gray signal constellation mapping is not necessarily the best option for the entire range of signal constellation rotation.

## I. INTRODUCTION

Wireless communication systems, current and emerging, use diversity in one form or another. It is well-known that diversity can mitigate the performance degradation caused by fading channels. An attractive option is signal space diversity (SSD), that can improve system performance without using extra bandwidth and power expansion [1]–[4]. The basic premise of SSD systems is that the rotated multidimensional signals constellations are used and the components of the signal constellation points are sent over independent fading channels. The independence of fading channels can be accomplished by the use of interleavers.

In literature, [1]–[3], the analysis on systems employing SSD is mostly limited to flat-fading channels. However, most channels are frequency-selective. In [4], an upper bound on pairwise error probability (PEP) by using Chernoff bound for an SSD system in frequency-selective channel was presented. The emphasis, however, was on the derivation of linear equalization techniques for SSD systems in frequency-selective channels. In this paper we present exact closed form expressions for pairwise error probabilities over frequency-selective fading channels for single symbol transmissions. Average probability of bit error ( $P_b$ ) is upper bounded by a union bound. It is shown that the upper bound is tight at high signal-to-noise ratios (SNR). The optimum rotation angles are found by minimizing the upper bound. The optimum rotation angles

vary as the number of diversity branches is increased. Furthermore, the effect of signal constellation mapping on the system performance is also presented and it is shown that the Gray signal constellation mapping is not necessarily the best option for optimal system performance over the entire range of signal constellation rotation.

The paper is organized as follows. Section II briefly outlines the main blocks of the system model. Section III presents the calculations of the upper bound of  $P_b$  for a system employing SSD in a multipath Rayleigh fading channel. Results are presented in Section IV, followed by the conclusions in Section V.

## II. SYSTEM MODEL

A system employing coordinate interleaving and constellation rotation is hereafter referred to as an “SSD system”. Furthermore, we confine ourselves to MPSK signal constellations and assume that perfect channel state information (CSI) is available at the receiver. A conventional MPSK signal constellation is denoted by  $\mathcal{S}_M = \{s_l = e^{j2\pi(l/M)} : l = 0, 1, \dots, M-1\}$ , where the energy has been constrained to unity and each symbol corresponds to  $m = \log_2 M$  bits. Anti-clockwise rotation over an angle  $\theta$  leads to the constellation

$$\mathcal{S}_M^\theta = \{s_l = e^{j(2\pi(l/M)+\theta)} : l = 0, 1, \dots, M-1\}. \quad (1)$$

The symbol mapper can be represented by a one-to-one mapping function  $\wp : \{0, 1\}^m \rightarrow \mathcal{S}_M^\theta, s = \wp(\mathbf{b})$ , where,  $\mathbf{b} = (b_1, \dots, b_m), b_j \in \{0, 1\}$  represents the binary sequence and  $s$  is chosen from the set  $\mathcal{S}_M^\theta$  consisting of  $M$  complex signal points. In case of  $N$  symbol transmission, let the sequence of rotated  $I$  and  $Q$  - components be denoted as  $\mathbf{x} = (x_0, x_1, \dots, x_{N-1})$  and  $\mathbf{y} = (y_0, y_1, \dots, y_{N-1})$ , respectively. Let  $\eta$  and  $\mu$  represent the  $I$  and  $Q$  interleavers, resulting in sequences  $\tilde{\mathbf{x}} = \eta(\mathbf{x}) = (\tilde{x}_0, \tilde{x}_1, \dots, \tilde{x}_{N-1})$  and  $\tilde{\mathbf{y}} = \mu(\mathbf{y}) = (\tilde{y}_0, \tilde{y}_1, \dots, \tilde{y}_{N-1})$ , respectively. The transmitted waveform for the rotated and interleaved system is given by

$$\begin{aligned} \tilde{s}(t) &= \sum_{i=0}^{N-1} \tilde{x}_i g(t - iT_s) \cos(2\pi f_c t) \\ &+ \sum_{i=0}^{N-1} \tilde{y}_i g(t - iT_s) \sin(2\pi f_c t), \end{aligned} \quad (2)$$

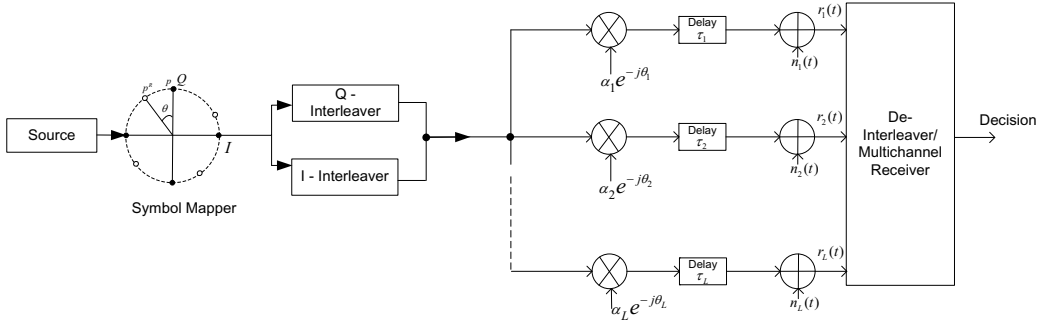


Fig. 1. Simplified block diagram of an equivalent baseband transmission model.

where

$$g(t) = \begin{cases} 1, & 0 \leq t \leq T_s, \\ 0, & \text{otherwise,} \end{cases}$$

$T_s$  is the symbol period and  $f_c$  is the carrier frequency.

The fading caused by a frequency-selective channel can be modeled as a linear filter characterized by a complex valued low pass equivalent impulse response [5],

$$h(t) = \sum_{l=1}^L \alpha_l e^{-j\theta_l} \delta(t - \tau_l),$$

where  $l$  is the path index,  $L$  is the number of resolvable paths,  $\delta(\cdot)$  is the Dirac delta function and  $\{\alpha\}_{l=1}^L$ ,  $\{\theta\}_{l=1}^L$  and  $\{\tau\}_{l=1}^L$  are the random channel amplitudes, phases and delays, respectively. As we assume that there is no cochannel interference, the transmitted signal is therefore, sent over  $L$  independent and identically distributed (i.i.d) slowly varying flat fading paths as shown in Figure 1. Furthermore similar to the analysis of multipath diversity in the literature, e.g., [5], [6], we assume, without loss of generality, the first channel with delay  $\tau_1 = 0$  to be the reference channel and  $\tau_1 < \tau_2 < \dots < \tau_L$ . Also, we assume that the sets  $\{\alpha\}_{l=1}^L$ ,  $\{\theta\}_{l=1}^L$  and  $\{\tau\}_{l=1}^L$  are mutually independent and are constant over at least a symbol interval. The transmitted signal after passing through the fading channel is perturbed by complex additive white Gaussian noise (AWGN) with a one-sided power spectral density of  $N_0$ . The AWGN noise is assumed to be independent of the fading amplitudes and statistically independent from channel to channel. The fading amplitudes,  $\{\alpha\}_{l=1}^L$ , are statistically independent random variables with a mean-square value  $\mathcal{E}[\alpha_l^2] = \Omega_l$ , described by a Rayleigh probability density function (PDF) given as [6]

$$p(\gamma_l) = \frac{1}{\bar{\gamma}} e^{-\frac{\gamma_l}{\bar{\gamma}}}, \quad (3)$$

where  $\gamma_l = \alpha_l^2 E_b / N_0$  is the SNR per bit per path and  $\bar{\gamma}$  is the average SNR per bit. Furthermore, it is important to state that if the various paths of a given impulse response are generated by different scatterers, they exhibit negligible correlation and hence it is reasonable to assume that  $\{\alpha\}_{l=1}^L$  are statistically independent random variables [7].

At the receiver we consider an  $L$ -branch maximum ratio combining (MRC) receiver. The performance of MRC receiver has been studied quite extensively in the literature

[5], [6]. MRC, regardless of the fading statistics on various diversity branches, is the optimal multichannel receiver since it results in a maximum likelihood (ML) detection [6]. As CSI is available at the receiver the channel phase shift at all the diversity branches can be removed without any error. Thus, after channel phase removal the samples are de-interleaved and the receiver performs an ML detection. At the output of the MRC the total conditional SNR per bit,  $\gamma_t$  of  $L$  i.i.d Rayleigh fading paths is given as [5], [6]

$$\gamma_t = \sum_{l=1}^L \gamma_l,$$

which has a chi-square PDF [5], [6]

$$p(\gamma_t) = \frac{1}{(L-1)! \bar{\gamma}^L} \gamma_t^{L-1} e^{-\frac{\gamma_t}{\bar{\gamma}}}. \quad (4)$$

### III. PERFORMANCE ANALYSIS OF SSD SYSTEM OVER RAYLEIGH FADING CHANNEL

A standard approach of evaluating the error probability of a signal set  $\mathcal{S}_M^\theta$  is based on the union bound [5]. The average probability of symbol error  $P_s$  is thus upper bounded by

$$P_s \leq P_s^{UB} = \frac{1}{M} \sum_{s \in \mathcal{S}_M^\theta} \sum_{\substack{\hat{s} \in \mathcal{S}_M^\theta \\ s \neq \hat{s}}} P(s \rightarrow \hat{s}), \quad (5)$$

where  $\mathcal{S}_M^\theta$  is the signal constellation of size  $|\mathcal{S}_M^\theta| = M = 2^m$  and  $P(s \rightarrow \hat{s})$  is the PEP that the receiver estimated  $\hat{s}$  when  $s$  was transmitted; given that  $s$  and  $\hat{s}$  are the only two signal constellation points under-consideration. The bound can be modified to evaluate the average bit error probability by considering the number of bits per symbol ( $m$ ) and the mapping rule specifying the Hamming distance associated with each PEP calculation [8]. Let  $a(s, \hat{s})$  represent the Hamming distance between the bit sequences of  $s$  and  $\hat{s}$  under consideration, then

$$P_b \leq P_b^{UB} = \frac{1}{m2^m} \sum_{s \in \mathcal{S}_M^\theta} \sum_{\substack{\hat{s} \in \mathcal{S}_M^\theta \\ s \neq \hat{s}}} a(s, \hat{s}) P(s \rightarrow \hat{s}). \quad (6)$$

In the literature, for the convenience of calculation the PEP is also approximated by using bounds (e.g., Chernoff bound [4]). We, on the other hand in the subsequent analysis, evaluate the exact PEP for MPSK signal constellations.

Coordinate interleaving is employed so that the  $I$  and the  $Q$ - channels experience independent fades. Let  $\gamma_{t1}$  and  $\gamma_{t2}$  be random variables with PDF given by (4). In order to calculate the average probability of error  $P_b$ , for a system employing coordinate interleaving, the conditional PEP needs to be averaged over the fading static, given as

$$P(s \rightarrow \hat{s}) = \int_0^\infty \int_0^\infty Q\left(\sqrt{(\gamma_{t1}d_I^2 + \gamma_{t2}d_Q^2)}\right) p(\gamma_{t1})p(\gamma_{t2})d\gamma_{t1}d\gamma_{t2}, \quad (7)$$

where  $Q(x)$  is the Gaussian  $Q-$  function defined as [5]

$$Q(x) = \frac{1}{\pi} \int_0^{\pi/2} e^{\frac{-x^2}{2\sin^2(\psi)}} d\psi, \quad x \geq 0 \quad (8)$$

and  $d_I^2$  and  $d_Q^2$  are the squared Euclidean distances between two different signal constellation points in the  $I$  and  $Q$ -directions, respectively. The distances are given as

$$\begin{aligned} d_I^2 &= (\cos(\varphi_1 + \theta) - \cos(\varphi_2 + \theta))^2, \\ d_Q^2 &= (\sin(\varphi_1 + \theta) - \sin(\varphi_2 + \theta))^2, \end{aligned} \quad (9)$$

where  $\varphi_1, \varphi_2$  represent the phases of the two signal constellation points under consideration, respectively. Using (4), (8) and the identity  $\Gamma(n) = (n+1)!$  [9] in (7), we simplify as

$$\begin{aligned} P(s \rightarrow \hat{s}) &= \frac{1}{\pi((L-1)!)^2 \bar{\gamma}^{2L}} \int_0^{\pi/2} \int_0^\infty \int_0^\infty \gamma_{t1}^{L-1} \\ &\quad e^{-\gamma_{t1}\left(\frac{2\sin^2(\psi)+\bar{\gamma}d_I^2}{2\sin^2(\psi)\bar{\gamma}}\right)} \gamma_{t2}^{L-1} \\ &\quad e^{-\gamma_{t2}\left(\frac{2\sin^2(\psi)+\bar{\gamma}d_Q^2}{2\sin^2(\psi)\bar{\gamma}}\right)} d\gamma_{t1}d\gamma_{t2}d\psi \\ &= \frac{1}{\pi} \int_0^{\pi/2} \left( \frac{\sin^2(\psi)}{\sin^2(\psi) + \frac{\bar{\gamma}d_I^2}{2}} \right)^L \\ &\quad \left( \frac{\sin^2(\psi)}{\sin^2(\psi) + \frac{\bar{\gamma}d_Q^2}{2}} \right)^L d\psi. \end{aligned} \quad (10)$$

For  $L = 1$ , (10) simplifies as

$$\begin{aligned} P(s \rightarrow \hat{s}) &= \frac{1}{2} - \frac{d_I^2}{2(2d_I^2 - C)} \left( \sqrt{\frac{\bar{\gamma}d_I^2}{2 + \bar{\gamma}d_I^2}} \right) + \\ &\quad \frac{C - d_I^2}{2(2d_I^2 - C)} \left( \sqrt{\frac{\bar{\gamma}(C - d_I^2)}{2 + \bar{\gamma}(C - d_I^2)}} \right), \end{aligned} \quad (11)$$

where  $C = d_I^2 + d_Q^2$ .

The largest diversity gain is achieved with  $L = 2$  [6], and for  $L = 2$  evaluation of (10) leads to (12). Using the results from [5] we can simplify (10) for any  $L$  as

$$\begin{aligned} P(s \rightarrow \hat{s}) &= \frac{\left(\frac{d_I^2}{d_Q^2}\right)^{L-1}}{2(1 - \frac{d_I^2}{d_Q^2})^{2L-1}} \left[ \sum_{k=0}^{L-1} \left(1 - \frac{d_Q^2}{d_I^2}\right)^k B_k \right. \\ &\quad D_k\left(\frac{\bar{\gamma}d_Q^2}{2L}\right) - \frac{d_I^2}{d_Q^2} \sum_{k=0}^{L-1} \left(1 - \frac{d_I^2}{d_Q^2}\right)^k J_k \\ &\quad \left. D_k\left(\frac{\bar{\gamma}d_I^2}{2L}\right) \right], \end{aligned} \quad (13)$$

where

$$\begin{aligned} B_k &= \frac{A_k}{\binom{2L-1}{k}}, \\ J_k &= \sum_{n=0}^{L-1} \frac{\binom{n}{k}}{\binom{2L-1}{n}} A_n, \\ A_k &= (-1)^{L-1+k} \frac{\binom{L-1}{k}}{(L-1)!} \prod_{\substack{n=1 \\ n \neq k+1}}^L (2L-n), \end{aligned}$$

and

$$D_k(c) = 1 - \sqrt{\frac{c}{1+c}} \left[ 1 + \sum_{n=1}^k \frac{(2n-1)!!}{n! 2^n (1+c)^n} \right],$$

with the double factorial notation  $(2n-1)!!$  denoting the product of only odd integers from 1 to  $2n-1$ .

#### IV. RESULTS & DISCUSSION

In the subsequent analysis we take QPSK signal constellation as an example signal constellation from MPSK and present a performance comparison of an SSD QPSK system with a conventional QPSK system. The  $P_b$  of a conventional QPSK system for multipath fading channel using MRC receiver is given as [5], [6]

$$P_b = \left( \frac{1-\mu}{2} \right)^L \sum_{l=0}^{L-1} \binom{L-1+l}{l} \left( \frac{1+\mu}{2} \right)^l, \quad (14)$$

where

$$\mu = \sqrt{\frac{\bar{\gamma}}{1+\bar{\gamma}}}.$$

The worst case scenario for a system employing constellation rotation and coordinate interleaving is when one branch has been completely removed, i.e.,  $d_I^2$  or  $d_Q^2 = 0$ . In such a case, (6) reduces to the performance of a conventional system.

##### A. Union Bound

In order to calculate (6) the squared Euclidean distances (SED) along  $I$  and  $Q$ - channels, for all possible symbol combinations, need to be calculated. Figure 2 shows the upper bound on the average probability of bit error  $P_b$  calculated by using (6) and by simulation for  $L = 1, 2$ , and 3 branch MRC receiver using SSD. The figure shows that the upper bound is tight at high SNR and is able to accurately predict the variation in  $P_b$  for the entire range of signal constellation rotation for different values of  $L$ . Gray labeled QPSK signal constellation is employed.

##### B. Optimal $\theta$

The optimum rotation angle  $\theta$  for  $P_b$  maybe found by minimizing (6). This can be accomplished by taking the derivative of the objective function (6) with respect to  $\theta$ . The derivative of (11) is given by (15), where  $d'_I = -\sin(\varphi_1 + \theta) + \sin(\varphi_2 + \theta)$ . Due to the limited space the derivatives of higher  $L$  are not included. The steepest descent algorithm is used to find the optimum angles for QPSK signal constellations. The optimum angle of  $\theta = 17.6^\circ, 15.4^\circ$  and  $14.4^\circ$  is calculated for  $L = 1, 2$ ,

$$\begin{aligned}
 P(s \rightarrow \hat{s}) = & \frac{1}{4(\frac{\bar{\gamma}}{2}(d_I^2 - d_Q^2))^3((\frac{\bar{\gamma}d_I^2}{2} + 1)(\frac{\bar{\gamma}d_Q^2}{2} + 1))^{3/2}} \left\{ -2(\frac{\bar{\gamma}d_Q^2}{2} + 1)^{3/2}(\frac{\bar{\gamma}d_I^2}{2})^{9/2} + 2\sqrt{\left(\frac{\bar{\gamma}d_I^2}{2} + 1\right)}\left(\frac{\bar{\gamma}d_Q^2}{2} + 1\right)^{3/2} \right. \\
 & (\frac{\bar{\gamma}d_I^2}{2})^4 + 3\sqrt{\left(\frac{\bar{\gamma}d_Q^2}{2} + 1\right)}\left(2(\frac{\bar{\gamma}d_Q^2}{2})^2 + \frac{\bar{\gamma}d_Q^2}{2} - 1\right)\left(\frac{\bar{\gamma}d_I^2}{2}\right)^{7/2} - 2\sqrt{\left(\frac{\bar{\gamma}d_I^2}{2} + 1\right)}\left(\frac{\bar{\gamma}d_Q^2}{2} + 1\right)\left(3(\frac{\bar{\gamma}d_Q^2}{2})^2 \right. \\
 & + 2(\frac{\bar{\gamma}d_Q^2}{2}) - 1\left.(\frac{\bar{\gamma}d_I^2}{2})^3 + 7(\frac{\bar{\gamma}d_Q^2}{2})(\frac{\bar{\gamma}d_Q^2}{2} + 1)^{3/2}(\frac{\bar{\gamma}d_I^2}{2})^{5/2} - \sqrt{\left(\frac{\bar{\gamma}d_I^2}{2} + 1\right)}(\frac{\bar{\gamma}d_Q^2}{2})\left(6(\frac{\bar{\gamma}d_Q^2}{2})^{5/2} - \right. \right. \\
 & 6\sqrt{\left(\frac{\bar{\gamma}d_Q^2}{2} + 1\right)}(\frac{\bar{\gamma}d_Q^2}{2})^2 + 7(\frac{\bar{\gamma}d_Q^2}{2})^{3/2} + 6\sqrt{\left(\frac{\bar{\gamma}d_Q^2}{2} + 1\right)}(\frac{\bar{\gamma}d_I^2}{2})^2 + \sqrt{\left(\frac{\bar{\gamma}d_I^2}{2} + 1\right)}(\frac{\bar{\gamma}d_Q^2}{2})^2\left(2(\frac{\bar{\gamma}d_Q^2}{2})^{5/2} \right. \\
 & - 2\sqrt{\left(\frac{\bar{\gamma}d_Q^2}{2} + 1\right)}(\frac{\bar{\gamma}d_Q^2}{2})^2 - 3(\frac{\bar{\gamma}d_Q^2}{2})^{3/2} + 4\sqrt{\left(\frac{\bar{\gamma}d_Q^2}{2} + 1\right)}(\frac{\bar{\gamma}d_Q^2}{2}) - 7\sqrt{\left(\frac{\bar{\gamma}d_Q^2}{2} + 1\right)} + 6\sqrt{\left(\frac{\bar{\gamma}d_Q^2}{2} + 1\right)} \right) \\
 & (\frac{\bar{\gamma}d_I^2}{2}) + \sqrt{\left(\frac{\bar{\gamma}d_I^2}{2} + 1\right)}(\frac{\bar{\gamma}d_Q^2}{2})^3\left(2(\frac{\bar{\gamma}d_Q^2}{2})^{3/2} - 2\sqrt{\left(\frac{\bar{\gamma}d_Q^2}{2} + 1\right)}(\frac{\bar{\gamma}d_Q^2}{2}) + 3\sqrt{\left(\frac{\bar{\gamma}d_Q^2}{2} + 1\right)} - \right. \\
 & \left. \left. 2\sqrt{\left(\frac{\bar{\gamma}d_Q^2}{2} + 1\right)}\right)\right\} \tag{12}
 \end{aligned}$$

and 3, respectively. In [2], the reported angle is  $22.5^\circ$  based on the nearest neighbor approximation and in [4], [10] for  $P_s$  the reported angle is  $\theta = 31.7^\circ$  for  $L = 1$ . For  $L = 2$ , in [4], the reported angle for  $P_s$  is  $\theta = 24^\circ$ .

#### C. Mapping Effect

Figure 3 shows the comparison of QPSK with Gray and Natural signal constellation mapping. The figure shows that Gray mapped signal constellation is not necessarily the best choice for the entire  $\theta$  range. At  $\theta = 0^\circ$ , for instance, Natural mapped signal constellation outperforms Gray mapped signal constellation. This provides a possibility to design signal constellation mapping for higher MPSK signal constellations which are capable of outperforming Gray signal constellation mapping at a wider range of  $\theta$ .

#### D. SSD Gain

Figures 4 and 5 show the comparison and the performance gain of an SSD system (6) over a conventional system (14) with multiple diversity branches. The simulation results are in good agreement with the closed form analytical expression (6). Figure 4 shows a gain of 10.7 dB for SSD over the conventional QPSK system at a bit error rate of  $3 \times 10^{-4}$  with  $L = 1$ . For  $L = 2$ , SSD systems shows a gain of 9.7 dB over the conventional QPSK system at a bit error rate of  $1 \times 10^{-6}$  as shown in the Figure 5. Furthermore simulation results commensurate the closed form expressions presented for an SSD system.

## V. CONCLUSIONS

In this paper, we have investigated the performance of a system employing signal space diversity using  $L$ -branch MRC receiver in a frequency-selective channel. An expression for the upper bound of  $P_b$  is derived for

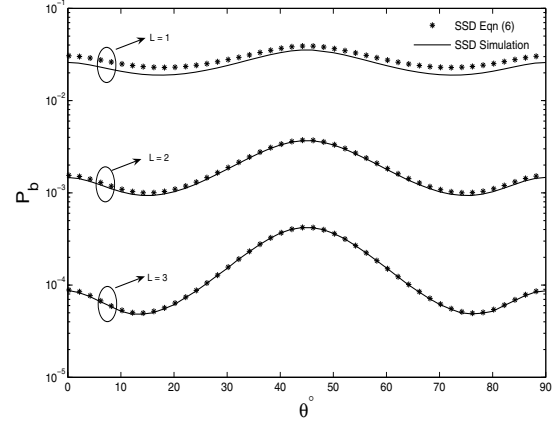


Fig. 2. Average probability of error  $P_b$  and  $P_b^{UB}$  versus rotational angle  $\theta$  of an SSD system using QPSK signal constellation over Rayleigh fading channel with perfect CSI at  $\bar{\gamma} = 8$  dB. Gray signal constellation mapping is used.

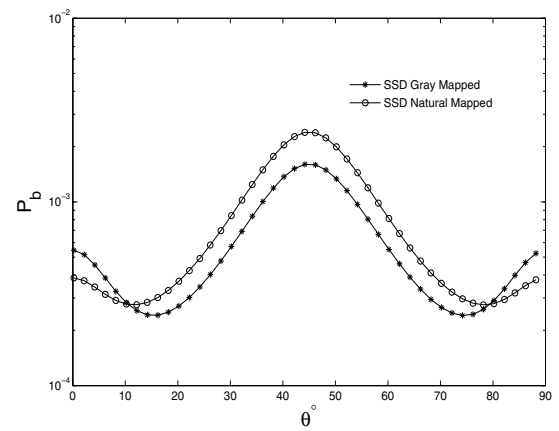


Fig. 3. Average probability of error  $P_b$  for Gray and Natural mapped QPSK signal constellation over Rayleigh fading channel with  $L = 2$  and perfect CSI at  $\bar{\gamma} = 10$  dB.

$$\begin{aligned} \frac{\partial P(s \rightarrow \hat{s})}{\partial \theta} = & - \left( d_I^2 \left( \frac{-2\bar{\gamma}^2 d_I^3 d'_I}{(2+\bar{\gamma}d_I^2)^2} + \frac{2\bar{\gamma}d_I d'_I}{2+\bar{\gamma}d_I^2} \right) \right) + \left( (C - d_I^2) \left( \frac{2\bar{\gamma}^2 d_I(C-d_I^2)d'_I}{(2+\bar{\gamma}(C-d_I^2))^2} - \frac{2\bar{\gamma}d_I d'_I}{2+\bar{\gamma}(C-d_I^2)} \right) \right) + \\ & \frac{2d_I^3 \sqrt{\frac{\bar{\gamma}d_I^2}{2+\bar{\gamma}d_I^2}} d'_I}{(-C + 2d_I^2)^2} - \frac{d_I \sqrt{\frac{\bar{\gamma}d_I^2}{2+\bar{\gamma}d_I^2}} d'_I}{-C + 2d_I^2} - \frac{2d_I(C - d_I^2) \sqrt{\frac{\bar{\gamma}(C-d_I^2)}{2+\bar{\gamma}(C-d_I^2)}} d'_I}{(-C + 2d_I^2)^2} - \frac{d_I \sqrt{\frac{\bar{\gamma}(C-d_I^2)}{2+\bar{\gamma}(C-d_I^2)}} d'_I}{(-C + 2d_I^2)} \quad (15) \end{aligned}$$

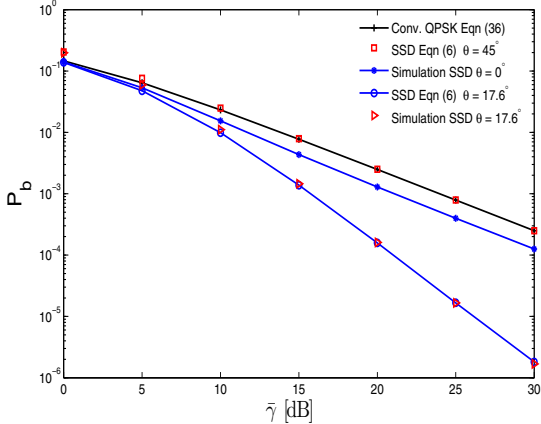


Fig. 4. Average probability of error  $P_b$  of conventional and SSD systems using QPSK signal constellation over Rayleigh fading channels with  $L = 1$  and perfect CSI. Gray signal constellation mapping is used.

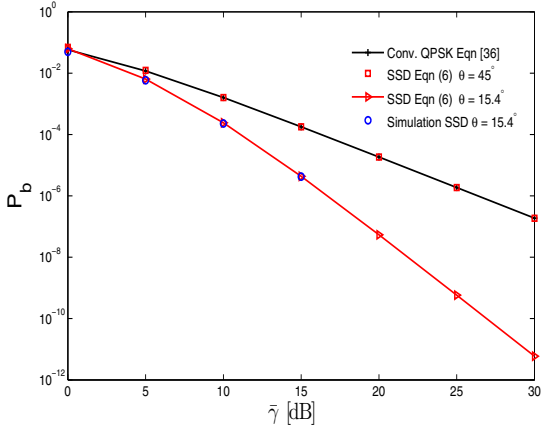


Fig. 5. Average probability of error  $P_b$  of conventional and SSD systems using QPSK signal constellation over Rayleigh fading channels with  $L = 2$  and perfect CSI. Gray signal constellation mapping is used.

MPSK signal constellations. The new derived bound is shown to be tight for the entire range of the constellation rotation angle at high SNRs. The optimum rotation angles are found by minimizing the upper bound. It is shown that the optimum rotation angles change as the diversity branches are increased. Furthermore, we have also shown that the Gray mapping in a system employing SSD is not necessarily the best option over the entire range of  $\theta$ .

#### ACKNOWLEDGEMENT

This work was supported by STW under McAT project DTC.6438.

#### REFERENCES

- [1] J. Boutros and E. Viterbo, "Signal space diversity: a power and bandwidth-efficient technique for the Rayleigh fading channel," *IEEE Trans. Information Theory*, vol. 44, no. 4, pp. 1453–1467, July 1998.
- [2] S. B. Slimane, "An improved PSK scheme for fading channels," *IEEE Trans. on Vehicular Tech.*, vol. 47, no. 2, pp. 703–710, May 1998.
- [3] N. F. Kiyani and J. H. Weber, "Iterative demodulation and decoding for rotated MPSK constellations with convolutional coding and signal space diversity," *IEEE 66<sup>th</sup> Vehicular Technology Conf.*, pp. 1712–1716, Oct. 2007.
- [4] R. Schober, L. H.-J. Lampe, W. H. Gerstacker, and S. Pasupathy, "Modulation diversity for frequency-selective channels," *IEEE Trans. Information Theory*, no. 9, pp. 2268–2276, Sept. 2003.
- [5] M. K. Simon and M. S. Alouini, *Digital Communication over Fading Channels - A Unified Approach to Performance Analysis*. New York, NY: John Wiley & Sons, 2000.
- [6] G. L. Stüber, *Principles of Mobile Communications-2nd ed.* Norwell, USA: Kluwer academic publishers, 2001.
- [7] H. Hashemi, "Impulse response modeling of indoor radio propagation channels," *IEEE Journal on Selected Areas in Comm.*, vol. SAC-11, pp. 967–978, Sept. 1993.
- [8] P. J. Lee, "Computation of the bit error rate of coherent M-ary PSK with Gray code bit mapping," *IEEE Trans. on Comm.*, vol. 32, no. 5, pp. 488–491, May 1982.
- [9] M. Abramowitz and I. A. Stegun, *Handbook of Mathematical Functions*. New York, NY: Dover Publications, 1972.
- [10] G. Taricco and E. Viterbo, "Performance of component interleaved signal sets for fading channels," *IEE Electronics Letters*, vol. 32, no. 13, pp. 1170–1172, April 1996.